

LNAPL Dissolution in Porous Media and Dissolution Rate Computations

Hatem Asal Gzar

Department of Environmental Engineering /College of Engineering/University of Baghdad.

Abstract

Benzene is the most toxic of the soluble components of gasoline. It is more mobile than the other aromatic hydrocarbons. Thus, benzene concentrations often determine the need for remedial action in contaminated sites. This paper aims to study the fate of dissolution and transport of benzene in saturated porous media and dissolution rate computations. A three dimensional bench-scale aquifer has been designed and constructed for this purpose. The experiments were conducted under unidirectional flow at different water flow velocities. The results characterized the dissolution behavior and distribution of an entrapped nonaqueous phase benzene source in a three dimensional aquifer model. The time invariant average mass transfer coefficient is determined at each interstitial velocity. The values of this coefficient ranged from 0.016 to 0.061 cm/hr. It is increased proportionally with velocity toward a limiting value. The results showed that the concentration of dissolved benzene reduces as the distance increased in x and/or z direction from the source of pollution. In most cases the concentration values were not stable with time at different values of the interstitial velocity. The dissolution rate of benzene in the aquifer is computed by two methods. The first method is taken from the effluent concentration and flow rate, the second is conducted by using Fick's first law. The resulted dissolution rates from the first method are higher than those of the second one.

Key words: Benzene, saturated porous media, dissolution, contamination, dissolution rate. computations.

Introduction:

Ground water contamination by nonaqueous phase liquids (NAPLs) originating from industrial and commercial activities is currently recognized as an important world-wide problem. Most of the NAPLs are organic solvents and petroleum hydrocarbons originated from leaking underground storage tanks, ruptured pipelines, surface spills, hazardous waste landfills, and disposal sites (Geller and Hunt, 1993; Seagren et al., 1993).

Upon release to the environment, NAPL (i.e., LNAPL or DNAPL) will migrate downward under the force of gravity. If a small volume of NAPL is released to the subsurface, it will move through the unsaturated zone where a fraction of the hydrocarbon will be retained by capillary forces as residual globules in the soil pores, thereby depleting contiguous NAPL mass until movement ceases. If sufficient LNAPL is released, it will migrate until it encounters a physical barrier (e.g., low permeability strata) or is affected by buoyancy forces near the water table. Once the capillary fringe is reached, the LNAPL may move laterally as a continuous, free- phase layer along the upper boundary of the water-saturated zone due to gravity and capillary forces. The migration may be in the direction of the maximum decrease in water table elevation, some migration may occur initially in other directions. A large continuous phase LNAPL mass may hydrostatically depress the capillary fringe and water table. Once the source is removed, mounded LNAPL migrates laterally, LNAPL hydrostatic pressure is removed, and the water table eventually rebounds. Infiltrating precipitation and passing ground water in contact with residual or mobile LNAPL will dissolve soluble components and form an aqueous-phase contaminant plume. In addition, volatilization may result in further spreading of contamination (Newell et al., 1995).

When the groundwater flow pass through the trapped ganglia or NAPL pools, a fraction of the NAPL dissolves in the aqueous phase and a plume of dissolved hydrocarbons is created. The dissolved NAPL concentrations may reach saturation or near saturation levels (Anderson et.al., 1992). The concentration of a dissolved NAPL in groundwater is governed mainly by interface mass-transfer processes that are often slow and rate limited (Mackay et.al., 1985; Powers et.al.,1991). The solubility represents the maximum concentration of the NAPL in water. (Newell et al, 1995).

Monoaromatic hydrocarbons such as benzene, toluene, ethylbenzene, and the three isomers of xylene (BTEX) are ground water pollutants commonly associated with petroleum product releases. The six BTEX compounds are depressants to the central nervous system, and chronic benzene exposure can cause leukemia (Federal register, 1985). Thus, contamination of potential drinking water sources by BTEX represents a serious threat to public health. The effective solubilities of BTEX compounds are lower than their single - compound aqueous solubilities. BTEX represent potential long-term sources for continued ground-water contamination at many sites (Newell et al, 1995; Phophi, 2004).

Only a limited number of experimental studies have focused on characterizing the NAPL dissolution process under three-dimensional flow conditions (Clement et al. 2004; Lee and Chrysikopoulos 2006).

The aim of the present research is to study the dissolution of benzene as a LNAPL in three dimensional homogeneous, isotropic, and saturated porous media.

Experimental setup:

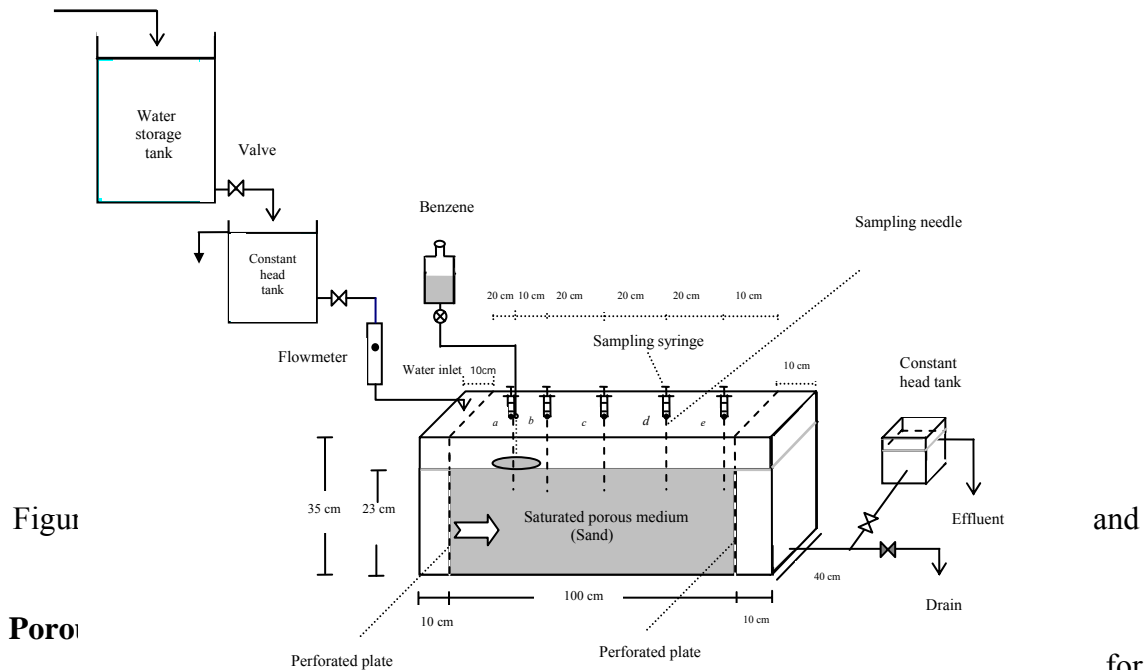
The dissolution experiments are conducted in a three dimensional intermediate-scale sand tank model. The tank is made of 1 cm thick Perspex plates with dimensions of 100 cm length, 40 cm width, and 35 cm height. Two perforated Perspex plates were used. Each plate was located 10 cm away from both sides dividing the tank into three chambers. The middle chamber was filled with saturated porous sand, and the chambers at both sides were filled with water to maintain constant heads. A filtration cloth is fixed on the perforated plates to prevent the sand from passing through the chambers at both sides of the aquifer. Figure (1) shows a schematic diagram of the laboratory-scale aquifer and the other auxiliary equipments. The auxiliary equipments consisted of a 125 liter storage tank contains tap water, two constant head reservoirs of 20 liter and 3 liter volumes, respectively, and a flowmeter (Cole-Parmer Instrument Co.; Chicago, Illinois 60648). A stream of 200 mg/l sodium azide solution was introduced to the influent water at the chamber in the left side of aquifer to inhibit biological growth.

Benzene Pool Formation:

In order to confine the LNAPL (benzene) pool at the surface of the experimental aquifer, a circular plastic bowl of 15 cm inner diameter and 5 cm height was used. The aquifer tank was filled with sand to a height of 23 cm and the water covers all the sand. The bowl was inversely placed on the upper surface of the water-saturated sand, so that the open side of the bowl was directly faced the sand. The aim of this configuration is to keep the pool within 15 cm of the porous media. The bowl was fixed by four screws with the Perspex cover of tank (figure 1). The LNAPL was colored with Sudan III which is a powder, nonvolatile organic dye of red color, soluble in hydrocarbons and insoluble in water. The red dye was added to assist the visual observation of the LNAPL pool. The thickness of the floating benzene pool in the bowl was 1 cm with solubility of 1770 mg/l. The benzene was injected to the pool at a rate of 18 ml/hr.

The sand of 1 mm particle size was packed into the tank at a height of 23 cm. This configuration resulted in a packed volume of about 92,000 cm³ (100×40×23 cm). The tank was filled with water (several cm above the upper level of sand) and left

overnight to settle and saturate the sand. The system was then flushed at maximum velocity until the effluent water was free of suspended fine material. After ending each experiment, the used sand was removed from the tank. The tank was washed and cleaned very well, and then filled with new sand to be prepared for a new experiment.



Figure

Porosity

for measurement of particle size distribution (by mechanical sieve analysis), porosity, as well as the permeability coefficient.

The particle size distribution was obtained by using mechanical sieve analysis as shown in figure (2). The uniformity coefficient (C_u), gives an indication of the range of grain sizes presented in a given soil sample. This coefficient was found to be 2.22 by using the following equation (Bowels, 1978; Al-Khafaji and Andersland, 1992):

$$C_u = \frac{D_{60}}{D_{10}} \quad (1)$$

where:

D_{10} : the effective size and represents the grain diameter corresponding to 10% passing.

D_{60} : the grain diameter corresponding to 60% passing.

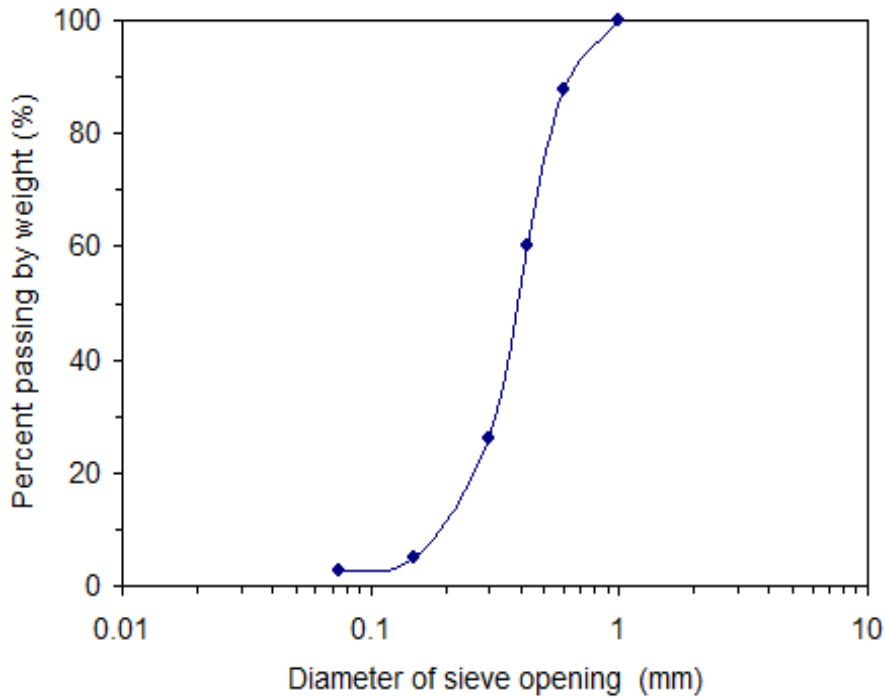


Figure (2): Particle size distribution curve for the Karbalaa's sand.

The porosity of sand is determined by measuring the weight of a sample of dry sand, the weight of the saturated sample submerged in water, the volume of sample, and temperature of the water by using the following equation:

$$n = \frac{v_v}{v} \quad (2)$$

$$v_v = \frac{W_s - W_d}{\rho_w} \quad (3)$$

where:

n = porosity.

v_v = voids volume (cm^3).

v = total volume of sample (cm^3).

W_s = weight of the saturated water sample (g).

W_d = weight of the dry sample (g).

ρ_w = density of the water (g/cm^3).

The bulk density of the dry sand was $1.6 \text{ g}/\text{cm}^3$. The porosity (n) of the porous medium was found to be 0.345.

The Interstitial velocity within the model aquifer was determined by using the following equation (Chrysikopoulos et al, 2000):

$$V_x = \frac{Q}{whn} \quad (4)$$

where Q is the water volumetric flowrate, w is the aquifer width, h is the head of water in the aquifer, and n is the porosity of porous medium. Five interstitial velocities were calculated using equation (4); the velocities are 0.90, 1.80, 2.34, 2.70, and 3.60 cm/hr.

Dissolution Experiments:

Five sampling ports (*a* to *e*) were conducted on the cover of sand tank. For collecting samples 15-gauged stainless-steel needles (manufactured by Sherwood Medical St. Louis, Mo, 63103 USA) were inserted into the ports and pushed into the porous medium. Wire inserted inside the needle during the placement process to prevent clogging.

Ten dissolution experiments were conducted in the three dimensional bench scale aquifer. These experiments were divided into two sets of samples; each one was collected from five selected points within the aquifer downstream from the LNAPL pool at a selected interstitial velocity. The first set was at depth $z = 1$ cm. The sampling points located at $(-7.5, 20, 1)$, $(2.5, 20, 1)$, $(22.5, 20, 1)$, $(42.5, 20, 1)$, and $(62.5, 20, 1)$, respectively. The second set of the samples were at depth $z = 3$ cm. The sampling points located at $(-7.5, 20, 3)$, $(2.5, 20, 3)$, $(22.5, 20, 3)$, $(42.5, 20, 3)$, and $(62.5, 20, 3)$, respectively. The sampling points $(-7.5, 20, 1)$ and $(-7.5, 20, 3)$ refer to sampling point below the LNAPL pool at depth 1 cm and 3 cm respectively. Five interstitial velocities of 0.90 , 1.80, 2.34, 2.70, 3.60 cm/hr were used.

The flow of water from the storage tank and the constant head tank was transferred by gravity. A flowmeter was used to measure the water flow from the constant head tank to the aquifer. For all experiments the flowrate was ranging from 5 to 20 ml/min. These flowrates yield an interstitial velocity ranged from 0.90 to 3.60 cm/hr. All experiments are conducted at temperature of $20 \pm 1^\circ\text{C}$. The water elevation in the aquifer was maintained at the desired level by using two constant head reservoirs; one before the inlet and the other after the outlet of the aquifer (Gzar , 2010)

Aqueous phase LNAPL concentrations were collected only when steady-state concentrations were observed at sampling port (*e*), which was the sampling port furthest away from the LNAPL pool. Interstitial water samples were collected from ports of the sand tank by using syringe-needles (figure 1). The volume of the used syringe is 5 ml. A 1 ml of sample was withdrawn from each location and stored in a glass vial, sealed with teflon-lined septa. The number of collected samples from the five ports in the porous medium was 200 samples at the depth of 1 cm, and 200 samples were at depth 3 cm from the top (figures 3). The samples were analyzed using Gas Chromatograph equipped with flame ionization detector (Gas Chromatograph GC-2014, Shimadzu Corporation, Analytical & Measuring Instrument Division, KYOTO, Japan).

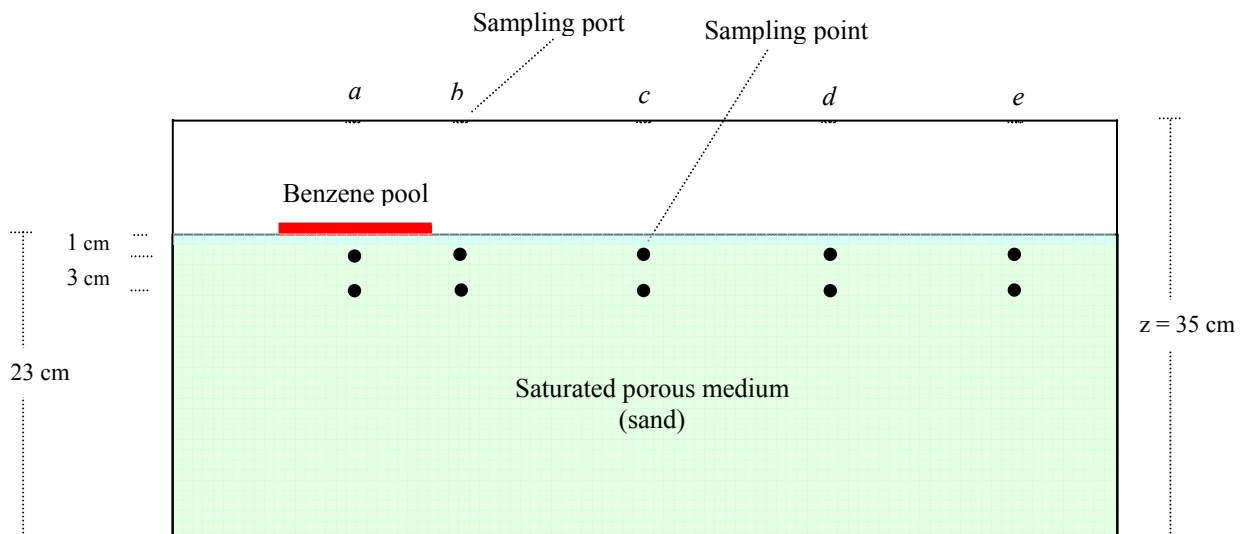


Figure (3): Sketch illustrate *side view* of the model aquifer sampling points location , the points located at the depths (z) of 1 cm and 3 cm.

Results and Discussion:

Figures 4a and 4b illustrate the distribution of benzene relative concentration (C/C_0) versus time at velocities of 0.90, 1.80, 2.34, 2.7, and 3.60 cm/hr at the depths of 1 cm and 3 cm respectively. The lateral distance (y) was 20 cm, and the concentration behavior was over 8 days. At both depths in porous media, the highest concentrations were observed at port *a*, sampling points (-7.5, 20, 1) and (-7.5, 20, 3), which was the closest sampling locations to the pool-water interface. Conversely, the lowest concentrations, in general, were observed at port *e* at sampling points (62.5, 20, 1) and (62.5, 20, 3) which were the farthest sampling locations.

Huntley and Beckett (2001) reported that the rate of dissolved-phase mass loss from dissolution of the LNAPL source compounds was simply the mass flux leaving the source area in the dissolved phase, which was the product of the groundwater flow rate and the concentration distribution provided from the LNAPL, both within and below the source zone. This groundwater pollutant flux occurs from the groundwater potentiometric surface (or corrected water table) to below the bottom of the LNAPL impacted interval (LNAPL/water interface).

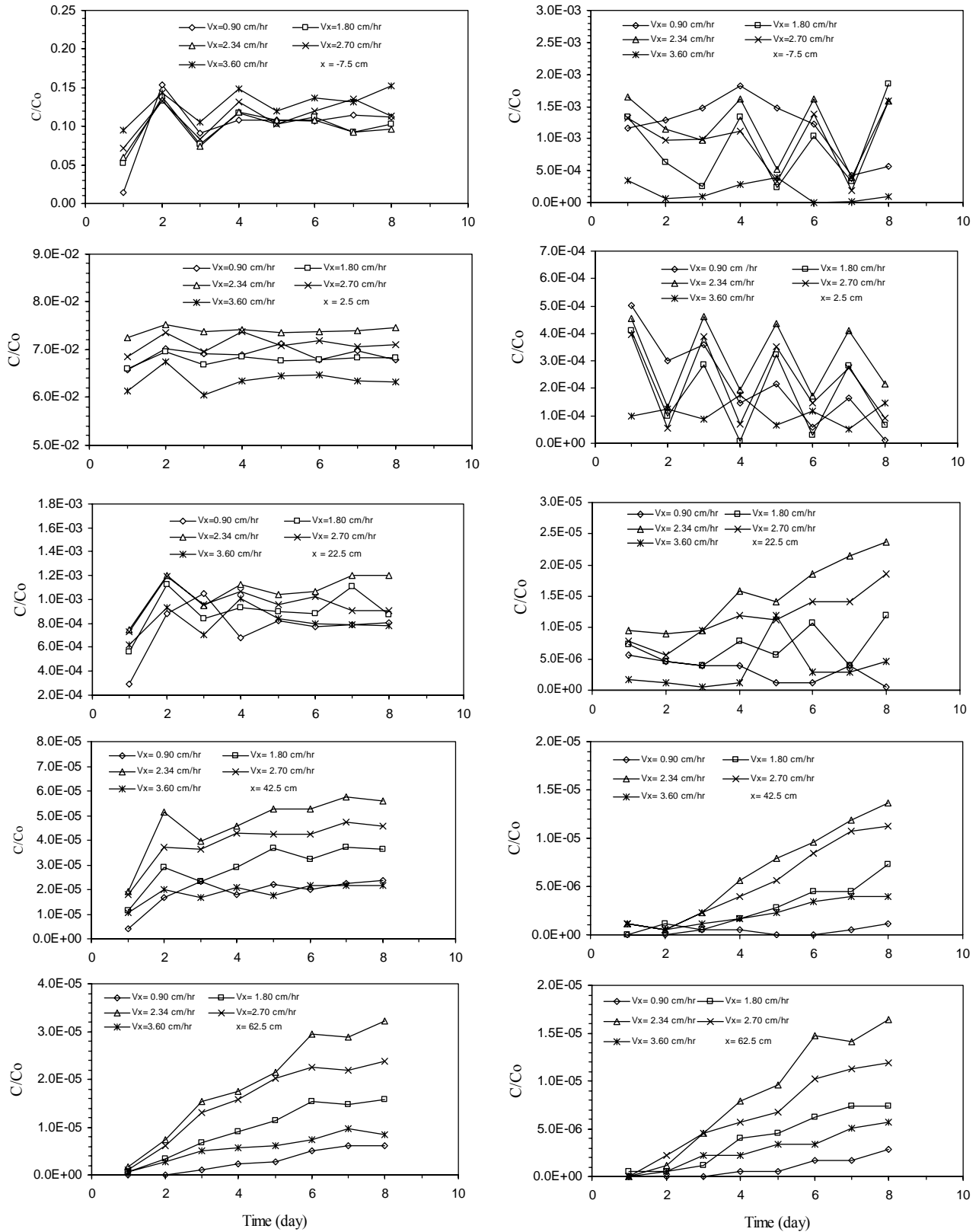
The period that an LNAPL source area provides dissolved phase at concentrations above some desired limit (the longevity of the source area) is a function of the original mass of the LNAPL of interest, their chemical properties, and the associated rate of dissolution of the LNAPL.

In general, it was observed that the relative concentrations are lower and farther away from the maximum relative concentration (C/C_0 equal to 1.0), and concentration did not reach the value of initial concentration 1770 mg/l (solubility of benzene) in the pool. The higher dissolution rates may be associated with: (1) higher interstitial velocity, (2) higher LNAPL saturation in the porous media, (3) increased contact area between LNAPL and water. Also there are several parameters affecting solubility including temperature, pH, cosolvents, dissolved organic matter, and dissolved inorganic compounds (salinity) (Newell et al., 1995). The solubility (C_s) is an important parameter that drives the rate of mass exchange processes.

Figures (5a) and (5b) show the change of the benzene relative concentrations with distance (x) at the depths (z) of 1cm and 3 cm respectively. These concentrations were below and downstream of the benzene pool at sampling times of 1 , 4 , and 8 day. The lateral distance y equals to 20 cm. The concentration values decreased with distance. In figure (5a), at time 1 day and at velocities equal or less than 2.7 cm/hr, the concentrations were increased within the distance -7.5 cm (below the pool-water interface) to 2.5 cm and then declined to the lower limits, while other profiles have the same behavior which are decreased with distance from upper to lower limits. In figure (5b) which shows the concentration versus distance at depth 3 cm, all concentration profiles decline with distance from upper to lower values except at velocity 3.60 cm/hr the concentration profile of time 8 day increase within the distance -7.5 cm to 2.5 cm and then continue to decline to the lower limit.

In figure (5a), approximately there is no significant difference between the concentration values at times 1 , 4 , and 8 day after horizontal distance (x) of about 2.5 cm. But in figure (5b), a significant difference in concentration can be noticed especially when the horizontal distance equals or less than 22.5 cm. The interpretation of this phenomenon is attributed to the effect of hydrodynamic conditions, and the horizontal and vertical (depth) distances which are collectively effect on the dispersion and transport of contaminant. Clement et.al. (2004) report that at high velocity, the net

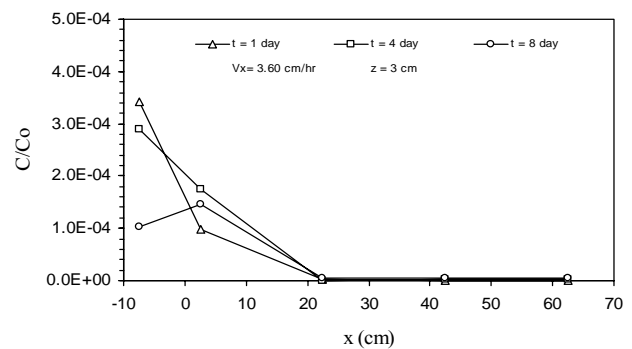
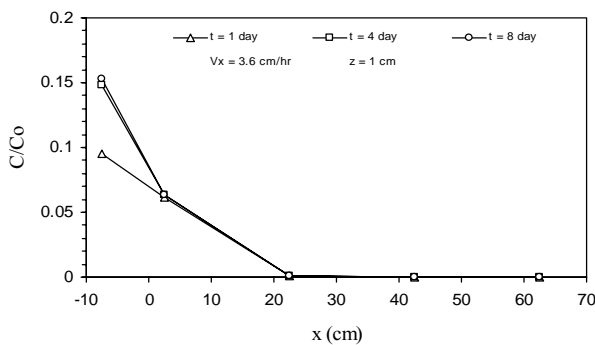
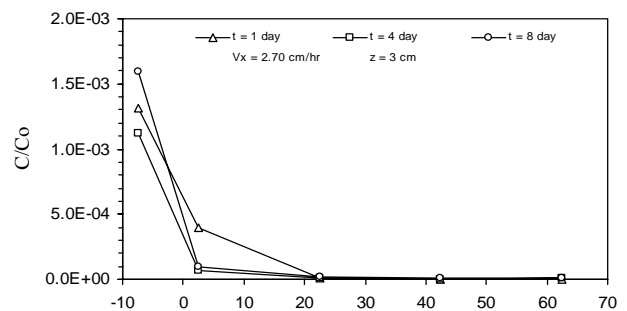
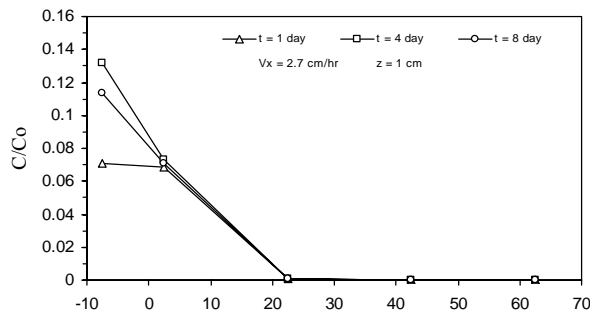
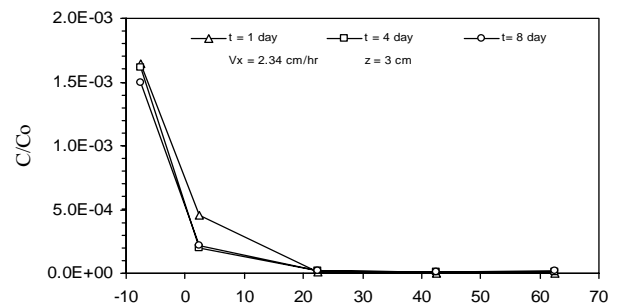
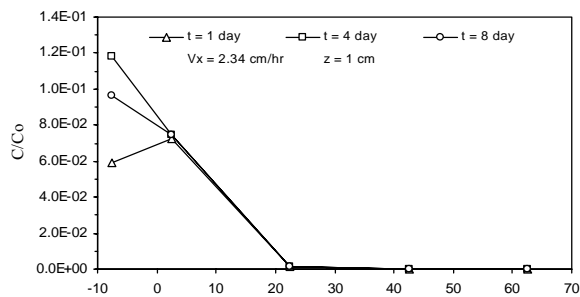
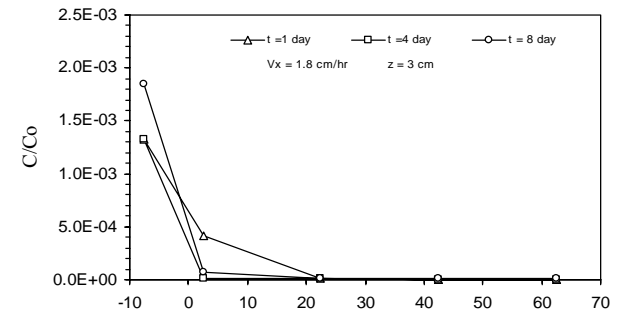
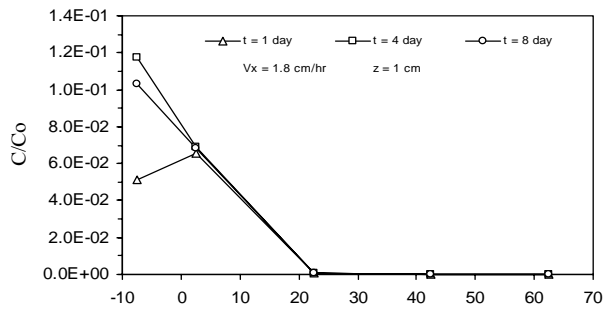
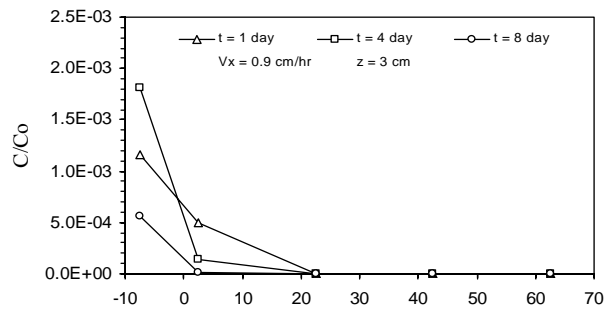
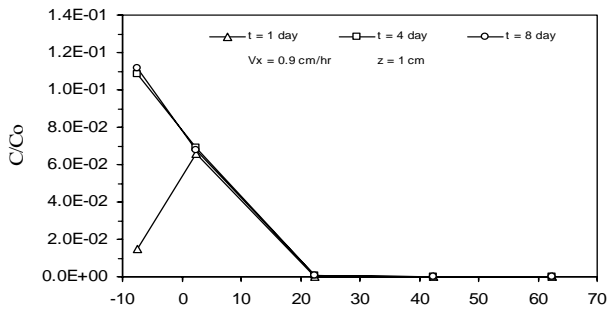
flow through the system will increase and therefore the overall dispersion and dilution rates will also increase. This should have a negative influence on the downstream concentration levels. On the other hand, the high velocity conditions will increase the overall dissolution rate because of the presence of high concentration gradient and better mixing conditions near the LNAPL-water boundary. This should have a positive influence on the downstream concentration levels. Further, high velocities also influence the time-dependent variations in the morphology of the LNAPL source. It is difficult to conceptualize the combined influence of all these complex processes that



(a)

(b)

Figure (4): The concentration of benzene versus time at different distance from the pool (x), at (a) depth (z) 1 cm, (b) depth (z) 3 cm, y = 20 cm



(a)

(b)

Figure (5): The benzene concentration versus distance from the pool (x) at Different interstitial velocities, y = 20 cm, and at depth (a) z = 1 cm, (b) z = 3 cm

Mass Transfer Coefficient Computations:

Time invariant, average mass transfer correlations for NAPL pool dissolution in saturated porous media were developed by Kim and Chrysikopoulos (1999), based on numerically determined average mass transfer coefficients evaluated for interstitial fluid velocities of 0.3,0.5,0.7, and 1.0m/day.

Chrysikopoulos and Kim (2000) reported that Johnson and pankow 1992; and Seagren et al., 1993 showed that the time required for complete pool dissolution is much longer than the contact time between the pool and the flowing ground water. Therefore, Chrysikopoulos and Kim (2000) estimate the mass transfer coefficients at steady state conditions.

Power and Heermann, 1999 report that the average mass-transfer coefficient (k^*) can be computed from the following equation:

$$k^* = n \sqrt{\frac{4D_z V_x}{\pi l_{c(e)}}} \tag{5}$$

where $l_{c(e)}$ is the characteristic length of pool. It is equal the square root of the pool area.

The time invariant average mass transfer coefficient (k^*) was experimentally determined by using equation (5) at each velocity. The vertical dispersion coefficients (D_z) was 2.84×10^{-2} , 5.53×10^{-2} , 6.96×10^{-2} , 7.80×10^{-2} , and 1.014×10^{-1} cm²/hr at the velocities 0.90, 1.80, 2.34, 2.70, 3.60 cm/hr, respectively (Gzar, 2010). Figure (6) indicates that k^* was proportional to the interstitial velocity (V_x). This behavior was attributed to increasing the concentration gradients at the NAPL-water interface with increasing V_x . The best fit relation of the time invariant average mass transfer coefficient (k^*) as a function to interstitial velocity (V_x) is:

$$k^* = 0.0166 V_x + 0.0016 \tag{6}$$

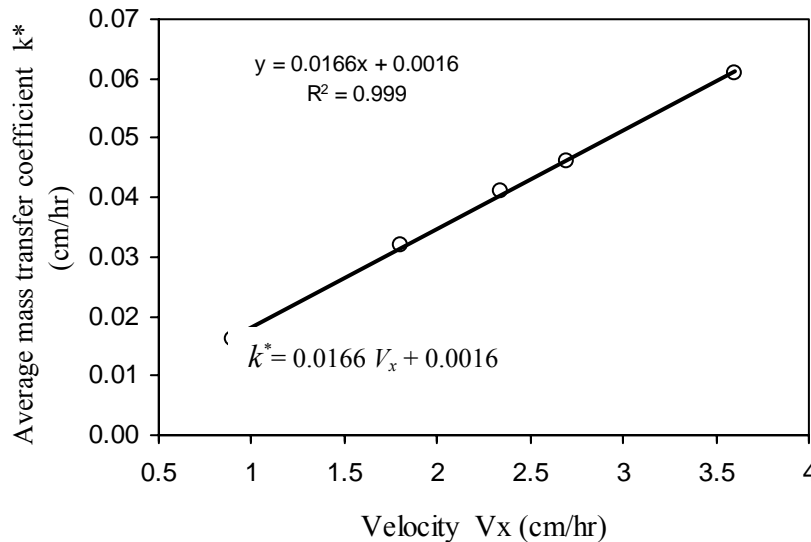


Figure (6): The relationship between average mass transfer coefficient (k^*)

and the interstitial velocity (V_x).

modified Sherwood number, $Sh(e) = k^* l_{c(e)} / D_e$, (figure 1), where D_e is the effective

molecular diffusion coefficient of the benzene. The computed $l_{c(e)}$, and D_e for the present research were 13.29 cm and $2.47 \cdot 10^{-2}$ cm²/hr, respectively.

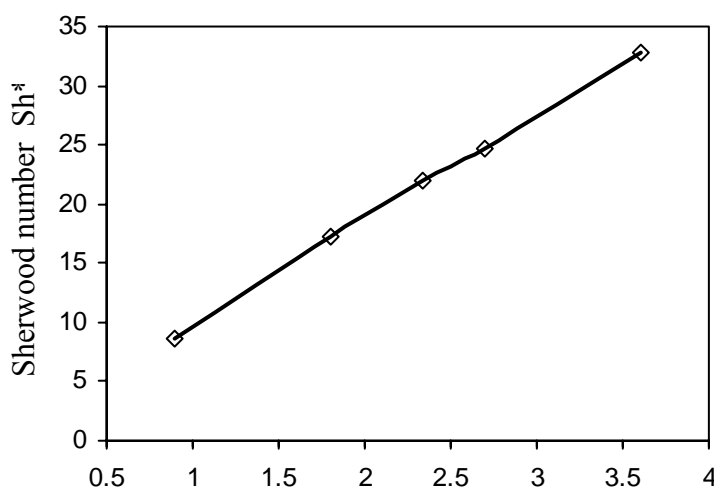


Figure (7): Modified Sherwood number $Sh^*_{(e)}$ behavior with the interstitial velocity (V_x).

Dissolution Rate Computations

The dissolution rate can be calculated from the following equation (Pearce et al., 1994):

$$R = \frac{dm}{dt} = QC_e \quad (7)$$

where

R = dissolution rate (mg/day),

Q = flow rate (l/day), and

C_e = benzene concentration in the effluent at steady state (mg/l).

Table (1) shows the calculated dissolution rate (R) for all conducted dissolution experiments at different interstitial velocities. The dissolution rate of benzene was determined by using equation (7). It was assumed that the steady state concentration at the farther distance 62.5 cm in the aquifer was equal to the effluent concentration. The dissolution rate was found in two cases, the first when depth (z) equals to 1 cm, and the second at $z=3$ cm. It was assumed that the same volume of benzene pool in calculations of dissolution rate. At experiments conducted, at depths 1 cm and 3 cm, the maximum mass loss from the pool or dissolution rate was about 24 mg over 8 day,

Pearce et al., 1994 assume that the dissolution rate of TCA and TCE remains constant and that the real dimensions of the pool do not change during the period of the dissolution process. But in fact the dissolution rate will decreased with time due to decreasing interfacial area, and an additional mass transfer limitation will result from downward shrinking of the pool with time. In the present research, the volume of pool was confirmed to be 177 cm³ by adding 18 ml/hr of benzene to the pool and the pool dimensions do not change with time, therefore a constant interfacial area will be achieved.

In equation (7), the resultant mass flux was the product of concentration and flow rate. From the discussion above, it was apparent that there were two components of groundwater mass flux from the LNAPL zone. One was from discrete water movement through the LNAPL at concentration equals to the maximum solubility, but with the flux scaled by the permeability toward water in that interval. The other

component of flux was due to dissolution and dispersion below the LNAPL zone, but the concentration decreases rapidly with depth below the bottom of the LNAPL impacted interval. The sum of the fluxes through and below the LNAPL source zone provides the net groundwater mass flux. Both the flux profiles below the LNAPL/water interface were polynomial, but for completely different reasons. The flux below the LNAPL/water interface was polynomially controlled by the permeability toward water. The flux below the LNAPL/water interface was controlled by the polynomial decrease in dissolved-phase concentrations. It can be seen that the maximum contaminant flux or maximum dissolution rate occurs at the LNAPL/water interface where the concentration was equal to the maximum solubility.

On the other hand, the dissolution rate (R) can be found using equation (8). The mass transfer coefficients (k^*) can be used to calculate the mass flux from the pool using Fick's first law (equation 8). The overall mass loss or dissolution from the pool can be calculated as the product of the flux and pool area (Barre et al., 2002).

$$R = \frac{dM}{dt} = -k^* C_s A \quad (8)$$

where:

A = interfacial area of the pool.

C_s = maximum concentration of benzene in the pool (solubility of benzene in water).

Equation (8) was used for five k^* values at five interstitial velocity. The maximum dissolution rate was about 3.67 mg over 8 day, and the average dissolution rate will be 0.295 gm/day.

Table (1) : Dissolution rate of benzene at different velocities.

V_x (cm/hr)	Q (l/day)	C_e at $z=1$ cm (mg/l)	C_e at $z=3$ cm (mg/l)	Dissolution rate (R) using equation (7) (mg/day)		k^* (cm/hr)	Dissolution rate (R) (mg/day) using equation (8)
				$z=1$ cm	$z=3$ cm		
0.90	19.872	0.011	0.005	0.219	0.099	0.016	0.120
1.80	39.744	0.028	0.013	1.113	0.517	0.032	0.241
2.34	51.667	0.057	0.029	2.945	1.498	0.041	0.308
2.70	59.616	0.042	0.021	2.504	1.252	0.046	0.346
3.60	79.488	0.015	0.01	1.192	0.795	0.061	0.459

Figure (8) shows a comparison between the dissolution rates computed by using equation (7) and those by using equation (8). At the depth (z) of 1 cm and 3 cm in porous media, the dissolution rate was increased with increasing flowrate and then decreased when the velocity equal or more than about 2.34 cm/hr. The concentrations at depth of 1cm in porous media were higher than those at depth 3 cm. This was due to the sampling points at depth 1 cm were closer to pool-water interface than those at 3 cm. The dissolution rates which is computed by using equation (8) give a linear relationship between the flowrate and dissolution rate, and the dissolution rate was lower than that of equation (7). It was increased with increasing velocity till reaching to a limiting value. The difference between the values of the two equation may be attributed to using

average mass transfer coefficient (k^*) values in equation (8) which was proportionally increased with velocity, while in equation (7) use a measured C_e values in calculation of dissolution rate. C_e values were increased with increasing flowrate but when the velocity reaches to 2.34 cm/hr the concentration will decreased. When implementing equation (7) for calculation of dissolution rate, the statistical analysis shows that polynomial correlations (equation 9 and 10) with correlation coefficients of .078 and 0.77 were found between the dissolution rate and water flow rate at depths 1 cm and 3 cm, respectively. A linear correlation (equation 11) was obtained with correlation coefficient 0.999 when equation (8) was used for calculating the dissolution rates. The results of dissolution rate when concentration values was used at the end of aquifer at $z = 3$ cm were more closer to that computed by Fick's first law (equation 8) than those at 3 cm depth (equation 7). This means, when the depth in porous media increased the dissolution rates will be approximately similar to those obtained by equation (8).

$$R = - 0.0019 Q^2 + 0.2069 Q - 3.3708 \quad (9)$$

$$R = - 0.0008 Q^2 + 0.095 Q - 1.5733 \quad (10)$$

$$R = 0.0057 Q + 0.0118 \quad (11)$$

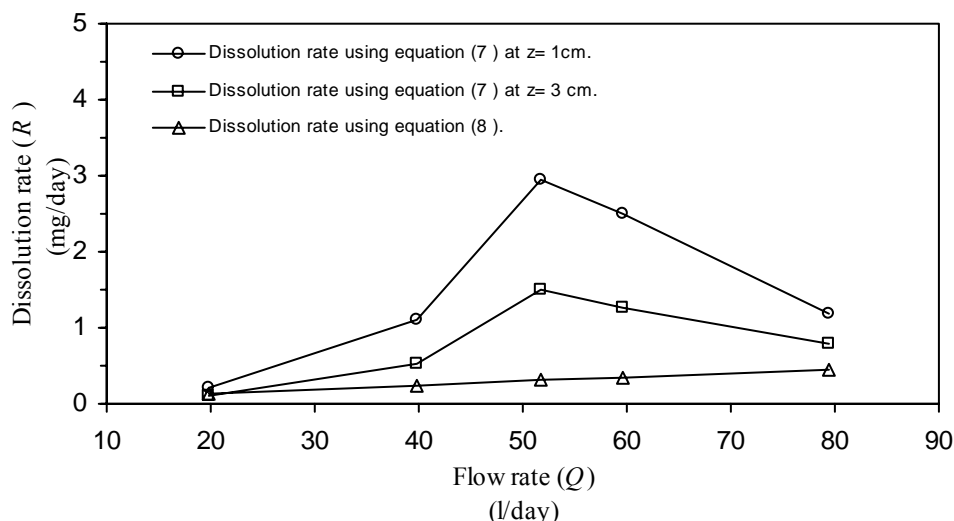


Figure (8): The dissolution rate of benzene versus volumetric flowrate of water.

Conclusions:

Three dimensional laboratory scale aquifer was constructed for dissolution experiments. The steady state concentrations were collected at ten locations, five locations were at depth 1 cm from the top surface of porous medium and the other five locations were at depth 3 cm. The time invariant average mass transfer coefficient was found at each interstitial velocity. The values of this coefficient were ranged from 0.016 to 0.061 cm/hr. It was increased proportionally with velocity toward a limiting value. The results show that the concentration of the LNAPL reduces as the distance increased in x and/or z direction from the source of pollution. In most cases, the concentration values decline with velocity more than 2.34 cm/hr at distances downstream of the LNAPL pool. The dissolved concentrations were higher at locations closer to the pool/water interface. LNAPL dissolution rate was determined using two methods, the first was taken from effluent concentration and flow rate, and the second method was accomplished by using Fick's first law.

References

- Anderson M.R., Johnson R.L., and Pankow J.F. , 1992, " Dissolution of dense chlorinated solvents into ground-water: 1. Dissolution from a well-defined residual source", *Ground Water*, 30 (2), 250-256.
- Al-Khafaji A.W., and Andersland O.B., 1992, "Geotechnical engineering and soil testing", Saunders College Publishing.
- Barre B.K.D., Harmon T.C., and Chrysikopoulos C.V. , 2002, " Measuring and modeling the dissolution of nonideally shaped dense nonaqueous phase liquid pools in saturated porous media", *Water Resour. Res.*, 38 (8).
- Bowles J.E., 1978, " Engineering properties of soils and their measurement ", McGraw-Hill Kogakusha, Ltd.
- Chrysikopoulos C.V., and Kim T-J, 2000, "Local mass transfer correlations for nonaqueous phase liquid pool dissolution in saturated porous media", *Transp. Porous Media*, 38, 167-187.
- Chrysikopoulos C.V., Lee K.Y., and Harmon T.C. , 2000, " Dissolution of a well-defined trichloroethylene pool in saturated porous media: Experimental design and aquifer characterization", *Water Resour. Res.*, 36 (7), 1687-1696.
- Clement T.P. , Kim Y.C., Gautam T.R., and Lee K.K, 2004, "Experimental and numerical investigation of DNAPL dissolution process in a laboratory aquifer model", *Journal of Ground water Monitoring & Remediation* , 24(4), 88-96.
- Federal Register (1985). November 13. U.S. Government Printing Office, Washington, D.C.
- Geller J.T. and Hunt J.R., 1993," Mass transfer from nonaqueous phase organic liquids in water saturated porous media", *Water Resour. Res.*,29(4), 833-845.
- Gzar H. A., 2010, "Experimental investigation and numerical modeling of benzene dissolution and transport in a saturated zone of the soil", Ph.D. thesis, College of Engineering/ University of Baghdad.
- Huntley D., and Beckett G.D., 2001, "Evaluation hydrocarbon removal from source zone: Tools to assess concentration deduction", The American Petroleum Institute.
- Hiscock K., 1995, "Ground-water pollution and protection", Environmental Science for Environmental Management, O'Riordan (eds).
- Kim T-J, and Chrysikopoulos C.V., 1999, "Mass transfer correlations for nonaqueous phase liquid pool dissolution in saturated porous media", *Water Resour. Res.* , 35 449-459.
- Lee K.Y. and Chrysikopoulos C.V., 2006, "Dissolution of a multicomponent DNAPL pool in an experimental aquifer", *Journal of Hazardous Materials*, B128, 218-226.
- Johnson R.L., and Pankow J.F., 1992, "Dissolution of dense chlorinating solvents into ground-water: 2. Source functions for pools and solvents", *Envir. Sci. and Tech.*, 26 (5), 896-901.
- Mackay D.M., Roberts P.V., Cherry J.A., 1985, "Transport of organic contaminants in ground-water: distribution and fate of chemicals in sand and gravel aquifers", *Environ. Sci. Technol.*, 19 (5), 384-392.
- Newell C.J., Acree S.D., Ross R.R., and Huling S.G., 1995, "Light nonaqueous phase liquids", EPA Ground Water Issue, EPA/540/S-95/500.
- Pearce A.E., Voudrias E.A., and Whelan M.P., 1994, "Dissolution of TCE and TCA pools in saturated subsurface systems", *Journal of Environmental Engineering*, 120 (5), 1191-1206.
- Phophi T.S., 2004, "The occurrence and evaluation of LNAPLs contamination in urban areas of South Africa", Master thesis, University of the Free State, Bloemfontein,

South Africa.

Powers S. E., Loureiro C. O., Abriola L. M., and Weber Jr. W. J., 1991, "Theoretical study of the significance of nonequilibrium dissolution of nonaqueous phase liquids in subsurface systems", *Water Resour. Res.*, 27(4), 463–477.

Power S.E. and Heermann S.E., 1999, " Potential ground and surface water impacts, appendix B: Modeling interface mass-transfer processes" presented in "A critical review: the effect of ethanol in gasoline on the fate and transport of BTEX in the subsurface", Editors Cannon G. and Rice D. , UCRL-AR-135949 Vol.4, chapter 2.

Seagren E.A., Rittmann B.E., and Valocchi A.J., 1993," Quantitative evaluation of flushing and biodegradation for enhancing in situ dissolution of nonaqueous phase liquids, *J. Contam. Hydrol.*, 12, 103-132.